OPEN

Light: Science & Applications (2015) 4, e300; doi:10.1038/lsa.2015.73

www.nature.com/lsa

ORIGINAL ARTICLE

A digitally generated ultrafine optical frequency comb for spectral measurements with 0.01-pm resolution and 0.7-μs response time

Yuan Bao[1,*], Xingwen Yi[2,*], Zhaohui Li[1], Qingming Chen[1,3], Jianping Li[1], Xudong Fan[4] and Xuming Zhang[3,5]

Optical spectral measurements are crucial for optical sensors and many other applications, but the prevailing methods, such as optical spectrum analysis and tunable laser spectroscopy, often have to make compromises among resolution, speed, and accuracy. Optical frequency combs are widely used for metrology of discrete atomic and molecular spectral lines. However, they are usually generated by optical methods and have large comb spacing, which limits the resolution for direct sampling of continuous spectra. To overcome these problems, this paper presents an original method to digitally generate an ultrafine optical frequency comb (UFOFC) as the frequency ruler for spectral measurements. Each comb line provides one sampling point, and the full spectrum can be captured at the same time using coherent detection. For an experimental demonstration, we adopted the inverse fast Fourier transform to generate a UFOFC with a comb spacing of 1.46 MHz over a 10-GHz range and demonstrated its functions using a Mach–Zehnder refractive index sensor. The UFOFC obtains a spectral resolution of 0.01 pm and response time of 0.7 μs; both represent 100-fold improvements over the state of the art and could be further enhanced by several orders of magnitude. The UFOFC presented here could facilitate new label-free sensor applications that require both high resolution and fast speed, such as measuring binding kinetics and single-molecule dynamics.
Light: Science & Applications (2015) **4,** e300; doi:10.1038/lsa.2015.73; published online 19 June 2015

Keywords: coherent detection; digital signal process; optical frequency combs; optical sensors; optical spectrometry

INTRODUCTION

Optical sensors and spectroscopic applications rely heavily on the measurement of various types of optical spectra, such as absorption/transmission spectra, fluorescence spectra, and Raman spectra,[1–4] but the resolution and speed are often a bottleneck. Among various available methods for spectral measurement, optical spectrum analysis (OSA) is the most popular. This method utilizes an optical grating or other dispersive element to spread different wavelength components to different spatial angles/locations and moves an optical detector (mounted with an aperture to adjust the resolution) to measure the intensities of different wavelength components. OSAs usually have fine spectral resolution (the best commercial equipment has $\delta\lambda$ ~0.001 nm), but the sweeping time is limited to approximately 0.01–2 s. Another widely used method is tunable laser spectroscopy,[5–7] which uses a tunable diode laser as the light source and a photodetector as the receiver. By varying the output wavelength of the tunable laser (usually a distributed feedback diode laser), the optical spectrum can be sampled point-by-point. This method can achieve high resolution (typically ~1 pm, but resolution as fine as 1 fm is possible) and fast speed (~1 ms–1 μs).[5,8,9] However, fast wavelength tuning by current injection or other methods often causes intensity noise, wavelength drift (typically 2 pm), and linewidth broadening,[10] and these problems offset most of the merits of this method. For this reason, OSAs are more popular than tunable laser spectroscopy for high-resolution spectral measurements, unless fast speed is the most important requirement. In this paper, we will use an OSA as the reference for the performance comparison.

Optical frequency combs (OFCs) have been widely used as precise frequency rulers in dimensional metrology, time keeping, and atomic/molecular spectroscopy.[11–13] However, they are often generated by optical methods, such as mode-locked lasers[14] and microresonators,[15] and the frequency spacing is usually large (e.g., 10 GHz in Ref. 14). These OFCs can be used to precisely measure discrete spectral lines of atomic/molecular transitions based on the beat notes.[11–13] However, the large frequency spacing of OFCs does not enable the use all of the comb lines as the sampling points to directly sample a continuous spectrum at the same time. Such sampling would yield low spectral resolution, e.g., 10 GHz corresponds to 0.08 nm at the wavelength of 1550 nm. Recently, sophisticated methods to overcome this limitation have been reported. For example, individual comb components can be

[1]Institute of Photonics Technology, Jinan University, Guangzhou 510632, China; [2]School of Communication and Information Engineering, University of Electronic Science and Technology, Chengdu 610051, China; [3]The Hong Kong Polytechnic University Shenzhen Research Institute, Shenzhen 518057, China; [4]Biomedical Engineering Department, University of Michigan, Ann Arbor, Michigan 48109, USA; and [5]Department of Applied Physics, Hong Kong Polytechnic University, Hong Kong S.A.R., China
*These authors contributed equally to this work
Correspondence: ZH Li, E-mail: li_zhaohui@hotmail.com; XM Zhang, Email: apzhang@polyu.edu.hk
Received 9 October 2014; revised 24 February 2015; accepted 12 March 2015; accepted article preview online 12 March 2015

tuned to scan over the frequency gap.[16–21] Other methods include spatially separating the comb lines using gratings,[21] Fourier transform spectroscopy of a single OFC[22] and dual-mode spectroscopy using two OFCs.[23,24] Nevertheless, few efforts have been made to decrease the comb spacing to improve the spectral resolution. This task may seem simple and straightforward, but it is challenging for conventional optical methods because the optical resonant cavity has to be very long, e.g., a mode spacing of 1 MHz requires a cavity length of 150 m. In the MHz range, electrical modulation is more suitable.

In this paper, we report original work in which we use digitally generated ultrafine optical frequency combs (UFOFCs) for high-resolution, fast spectral measurements. The basic idea is to digitally generate an electrical waveform to modulate a continuous-wave (CW) laser beam into the UFOFC, which is then used as the probing light for the optical sensors; the output spectrum is detected by a coherent receiver. The generation of the UFOFCs is based on our recent work that used an advanced digital signal processing (DSP) technique,[25–27] which can control the frequency spacing of comb from sub-MHz to several hundred MHz. Conceptually, the use of UFOFC for spectral detection in optical sensors yields three prominent benefits. First, the frequency spacing of the comb can reach the sub-MHz level, which enables discernment of spectral shifts of as little as 10^{-5} nm. Compared with the 0.001-nm resolution of OSAs, this spacing is already an improvement of two orders of magnitude. Second, the DSP in the current setup takes only 0.7 μs to complete one measurement run, which represents an improvement in the response speed of four orders of magnitude compared with the typical sweeping time 0.01–2 s of the OSAs. Finally, all the comb lines are retrieved by the coherent receiver and simultaneously computed by digital processing, thus enabling one to capture the full optical spectrum at a single time point with a high signal-to-noise ratio. The aim of this work is to explore the great opportunity of UFOFCs for high-resolution, fast optical spectral measurements using a simple experiment.

MATERIALS AND METHODS

Conceptual design

A conceptual diagram is shown in Figure 1. A user-defined train of 1 and 0 data is transformed by the inverse fast Fourier transform (IFFT) before being applied to an electric-to-optical (E/O) modulator to modulate the narrow–linewidth CW laser into the UFOFC (see Supplementary Section S1 for details). When the UFOFC passes the device under test (DUT), the optical properties of the sample (specifically, the changes in amplitude, phase, and polarization of each comb line) are recorded. A coherent receiver measures the amplitude and phase information of the optical signals after the optical-to-electrical (O/E) conversion and finally sends the signals to the computer for data process using a fast Fourier transform (FFT). Figure 1a presents the generated UFOFC. Figure 1b and 1c shows the altered frequency comb after the DUT and the calculated optical spectrum after data processing, respectively.

Experimental setup

For experimental demonstration, we set up the whole system for UFOFC generation and detection as shown in Figure 2. In the computer, the data train is carefully chosen to have an equal-amplitude, pseudo-random phase relationship,[25–27] and its IFFT has all real values. The digital output is then uploaded into an arbitrary waveform generator (AWG, Tektronix 7122B) for conversion into analog electrical signals. The IFFT has a data length of 8192 points, and the waveforms produced by the AWG are continuously output at 12 GSamples/s. It is noted that the pseudo-random phase relationship is fixed once it is generated. Here, the 'pseudo-randomness' is used to reduce the peak-to-average power ratio of the signal in the time domain to ease the requirements for the intensity modulator and the photodetector (see Supplementary Section S2 for details). Uploading of IFFT data to the AWG is needed only the first time; after uploading, the AWG can store the IFFT data, and it then outputs the

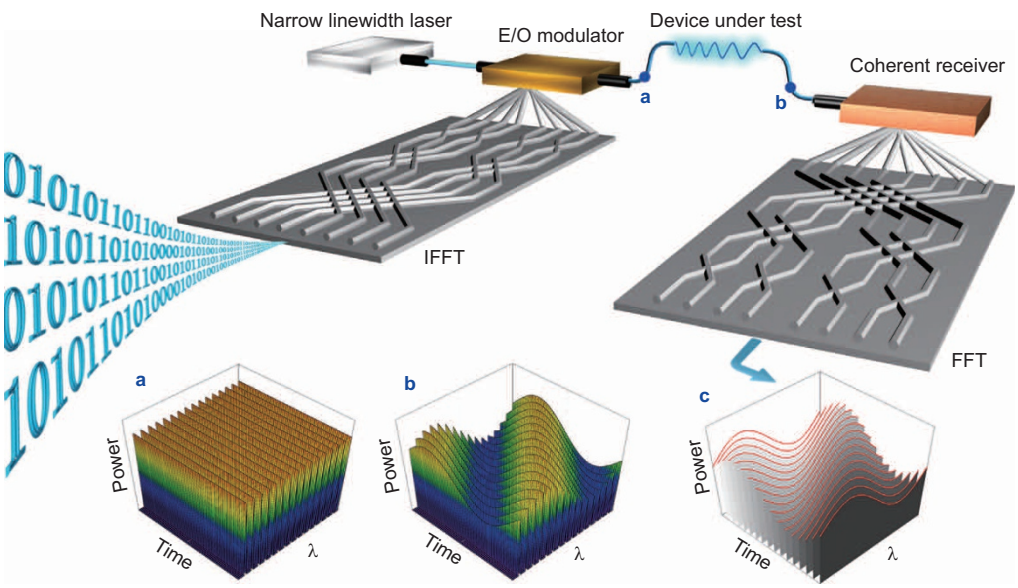

Figure 1 Conceptual design of the optical sensing method using the digitally generated UFOFC and the DSP technique. A user-defined proper train of 0 and 1 is subject to the IFFT, which is then used to modulate the input laser into a UFOFC (see inset **a**). After the UFOFC passes the device under test (DUT), the optical properties of the DUT are encoded in the changes of amplitude, phase and/or polarization of each comb line (see inset **b**). The coherent receiver detects the changes using the coherent detection technique, whose analog electrical outputs are sampled and sent to the computer for data processing using the FFT algorithm. The obtained spectrum is shown in inset **c**.

doi:10.1038/lsa.2015.73

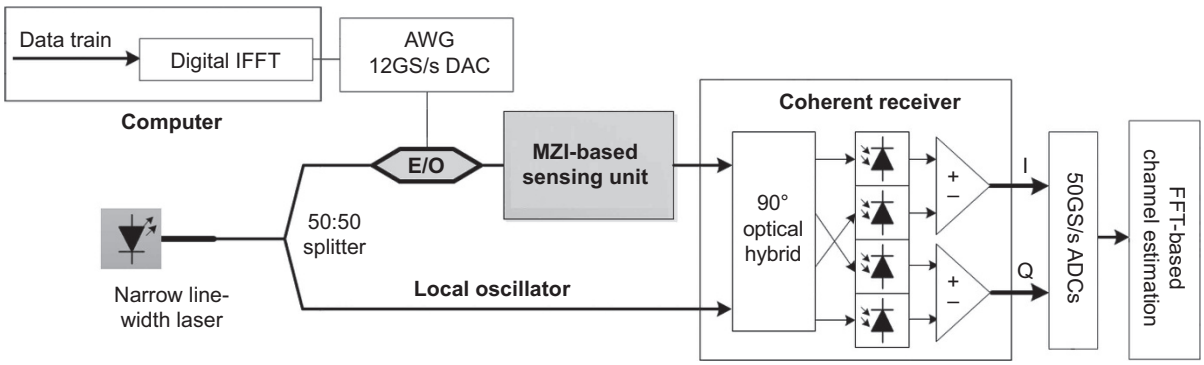

Figure 2 Experimental diagram of the sensing system using the digitally generated ultrafine optical frequency comb and coherent optical detection. ADC, analog-to-digital converter; DAC, digital-to-analog converter.

corresponding waveforms periodically, without the need for further input from the computer. This procedure greatly simplifies the UFOFC generation. For optical signals, a CW fiber laser with a wavelength of 1550 nm and very narrow linewidth of approximately 400 Hz is used as the input. The laser is split into two branches: one goes directly to the coherent receiver to act as the local oscillator, and the other is modulated by the electrical signals from the AWG to generate the UFOFC. Because the data sequence after the IFFT is intentionally designed to be real-valued, amplitude modulation is sufficient for this experiment. The UFOFC passes the sensing unit and enters the coherent receiver (Picometrix CR-100A, bandwidth 25 GHz) to mix with the local oscillator for coherent detection. The output of the coherent receiver is sampled at 50 GSamples/s by a real-time oscilloscope (Tektronix 72004B), which feeds the data into the computer for computing the optical spectrum using an FFT-based channel estimation algorithm.[26]

Generated ultrafine optical frequency comb

The power spectrum of the generated UFOFC is shown in Figure 3. It is measured using the coherent detection system presented in Figure 2 without the sensing unit. In Figure 3, most of the power is distributed in the range of $\Delta f = -5$ to $+5$ GHz. The power at 5 GHz is <2 dB less than that at 0 GHz. The zoomed view in Figure 3 shows that the comb lines are spaced by 12 GHz/8192 = 1.46 MHz (≈0.01 pm at λ = 1550 nm). The comb spacing could be further reduced by increasing the length of IFFT. In this experiment, the AWG has a sampling rate of 12 GSamples/s. Thus, it can generate a frequency comb in the range of 0 to +6 GHz, as limited by the Nyquist sampling theorem. The power spectrum in the −6 to 0 GHz range is symmetric with that in 0 to +6 GHz range. In total, the maximum bandwidth of the frequency comb is −6 GHz to +6 GHz. Nevertheless, in the comb generation process, the power densities from −6 to −5 GHz and from +5 to +6 GHz are intentionally set to 0, which helps improve the noise resistance capability. In this manner, a low-noise, stable UFOFC with a comb spacing of 1.46 MHz over the range of 10 GHz is generated. Some additional experimental data regarding the UFOFC, such as the time-domain waveform and the overlapped power spectra of 100 measurements, are shown in Supplementary Section S2.

Mach–Zehnder refractive index sensing unit

For measurement of real samples, we built a refractive index sensing unit based on the unbalanced Mach–Zehnder interferometer (MZI) (see Figure 4). The DUT uses a quartz cuvette to contain liquid samples. In this experiment, we introduced a subtle change of refractive index by slightly varying the temperature of the liquid sample. Here, an MZI is used because of its simplicity and its broad use in refractive

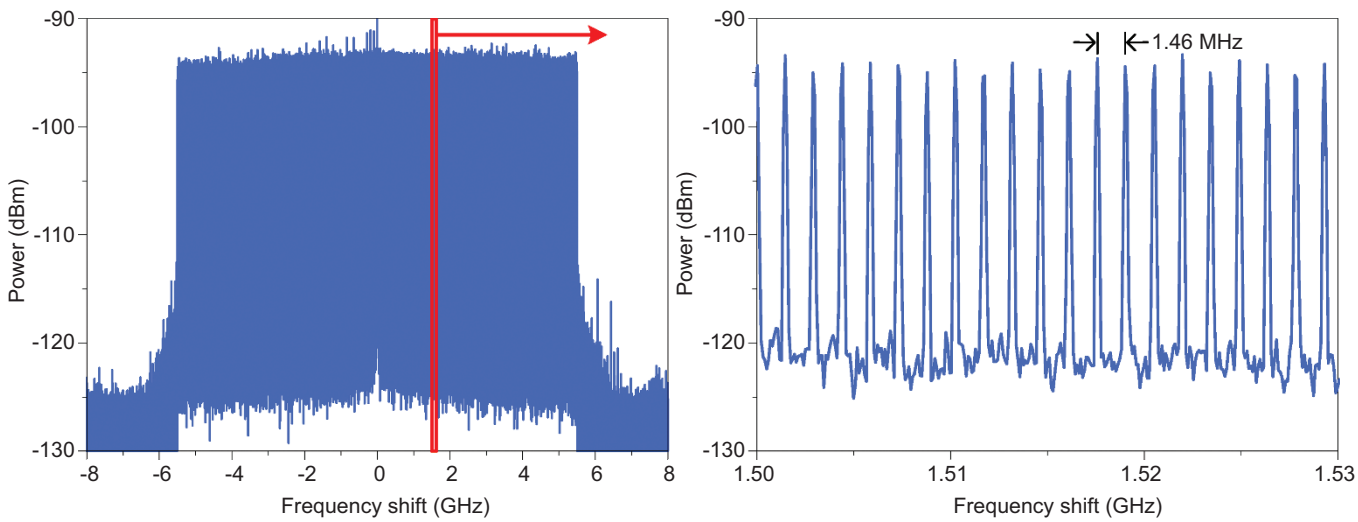

Figure 3 Power spectrum of the generated ultrafine optical frequency comb with a frequency spacing of 1.46 MHz.

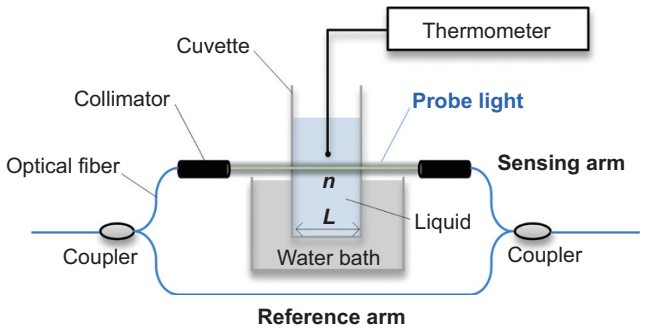

Figure 4 Diagram of the refractive index sensing unit using the unbalanced Mach-Zehnder interferometer. It consists of two fiber couplers and two optical arms with different lengths. The reference arm is simply a short section of fiber, and the sensing arm utilizes a pair of collimators to guide the probe light through the liquid sample contained in a quartz cuvette. The quartz cuvette is put in a water bath, whose temperature is controlled by an electric heater. Slight variation of the temperature of the liquid sample introduces a subtle change in the refractive index of the liquid sample. As a result, the phase and peak wavelength of the transmitted light are shifted.

index sensors based on measurement of the spectral shifts of transmission peaks.[28–33] The phase difference between the sensing arm and the reference arm of the MZI can be expressed as

$$\phi = \frac{2\pi}{\lambda}\left(n\mathrm{L} + \mathrm{OPD}_{i0}\right) \quad (1)$$

where λ is the wavelength, n is the refractive index of the sample, L is the physical length of the liquid sample along the optical axis, and OPD_{i0} represents the optical path difference (OPD) from all the other parts (e.g., fibers and collimators) except for the DUT. When the temperature is varied to induce a refractive index change Δn in the sample, the phase change $\Delta\Phi$ and the shift in the peak wavelength $\Delta\lambda$ can be expressed as

$$\Delta\Phi = \frac{2\pi\mathrm{L}}{\lambda}\Delta n \quad (2)$$

$$\Delta\lambda = \frac{\lambda\mathrm{L}}{\mathrm{OPD}_0}\Delta n \quad (3)$$

Here, $\mathrm{OPD}_0 = n_0 L + \mathrm{OPD}_{i0}$ is the initial total OPD between the sensing arm and the reference arm, and n_0 is the initial refractive index of the sample (see Supplementary Section S3 for the derivations of these equations).

RESULTS AND DISCUSSION

Comparison of the spectral resolutions

In the experiment, we used ethanol as the sample liquid and examined the change of its refractive index with temperature using both the OSA method and the UFOFC method. Here, the OSA method refers to using an OSA (Yokogawa AQ6370B, which can achieve a resolution of 0.002 nm) to measure the transmission spectra. The measured transmission spectra of the MZI sensing unit are presented in Figure 5. As the phase is increased, the spectrum is shifted to higher frequencies. The period is $\Delta F = 5.4961$ GHz, which implies that the initial OPD is $\mathrm{OPD}_0 = 0.05455$ m.

Figure 6 shows the peak shift determined using the OSA method and the measured phase change determined using the UFOFC method when the temperature is changed by only 0.1 ℃ (from 24.4 to 24.5 ℃). The OSA method measures only four data points of spectral shift,

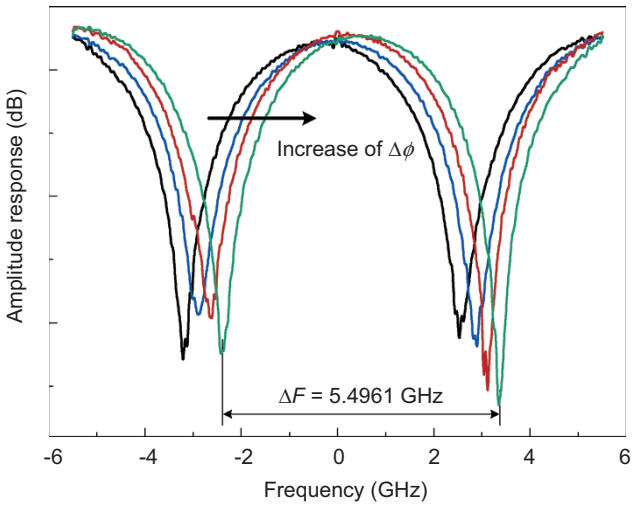

Figure 5 Measured transmission spectra of the Mach–Zehnder interferometer sensor when ethanol is used as the sample liquid. The spectrum is blueshifted with a larger optical phase. The period is $\Delta F = 5.4961$ GHz, which indicates that the initial optical path difference OPD_0 between the two arms is 0.05455 m.

whereas the UFOFC method produces many more. This difference occurs because the OSA has a resolution that is limited to $\delta\lambda = 0.002$ nm and thus cannot discern very small changes in the refractive index and temperature ($\delta n = 1.4 \times 10^{-5}$, $\delta T = 0.033$ ℃). By contrast, the UFOFC has a phase resolution of $\delta\phi = 0.0017$ rad (which is determined by the comb spacing of 1.46 MHz) and can detect much smaller changes ($\delta n = 8.4 \times 10^{-8}$, $\delta T = 2.0 \times 10^{-4}$ ℃). The resolution of the UFOFC method is finer than that of the OSA method by a factor of 167. Similarly, the UFOFC method is 167 more sensitive than the OSA method in terms of the refractive index change and the temperature change. Table 1 presents the resolutions of the OSA method and the UFOFC method for different parameters (see Supplementary Section S4 for the details of the resolution calculations).

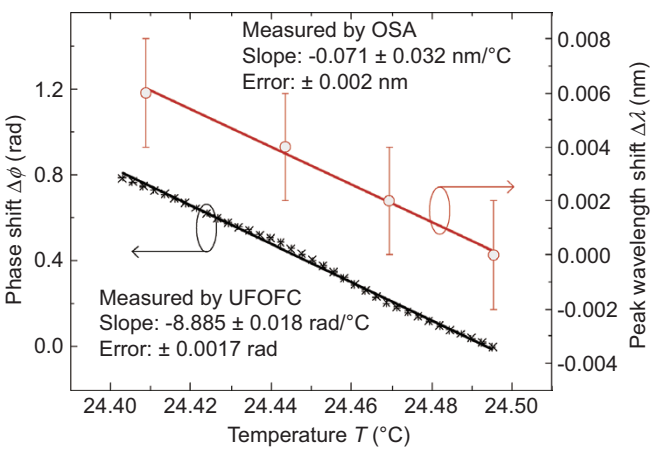

Figure 6 The phase change (black crosses) measured using the UFOFC method and the peak shift (red dots) measured using the OSA method when the ethanol sample is heated up from 24.4 to 24.5 ℃. Within the temperature change of 0.1 ℃, the OSA method discerns only 4 data points, with a large error (±0.002 nm), whereas the UFOFC method produces 36 data points, with a very small error (±0.0017 rad). For the phase shift data points, the error bars are too small to see.

doi:10.1038/lsa.2015.73

Table 1. Comparison of the resolutions of the OSA method and the UFOFC method

	The OSA method	The UFOFC method	Ratio (OSA over UFOFC)
Measured parameter	Peak wavelength shift	Phase shift of comb lines	
Resolutions			
Phase shift $\delta\phi$	–	0.0017 rad	
Wavelength shift $\delta\lambda$	0.002 nm	0.01 pm	167
Refractive index change δn	1.4×10^{-5}	8.4×10^{-8}	167
Temperature change δT	0.033 ℃	2.0×10^{-4} ℃	167

Table 2. List of the thermo-optic coefficients of ethanol measured by different methods

	Thermo-optic coefficient of ethanol dn/dT ($℃^{-1}$)	Error	Measured conditions
OSA method	$(-4.9 \pm 2.2) \times 10^{-5}$	45%	24.5 ℃, 1550 nm
UFOFC method	$(-4.328 \pm 0.009) \times 10^{-4}$	0.2%	24.5 ℃, 1550 nm
Fresnel reflection method	$(-4.28 \pm 0.08) \times 10^{-4}$	1.8%	18–56 ℃, 1550 nm
Fiber Bragg grating[34]	$(-3.99 \pm 0.20) \times 10^{-4}$	5.0%	21.0 ℃, 1550 nm

Comparison of the measured thermo-optic coefficients

From the slopes and the error ranges of the curves in Figure 6 and using Equations (2) and (3), the thermo-optic coefficient (TOC) of ethanol is calculated to be $dn/dT = (-4.9 \pm 2.2) \times 10^{-4}$ ℃$^{-1}$ by the OSA method and $(-4.328 \pm 0.009) \times 10^{-4}$ ℃$^{-1}$ by the UFOFC method. The error is an intolerable 45% for the OSA method, but it is only 0.2% for the UFOFC method, which demonstrates that the UFOFC is more precise than the OSA method by a factor of 225. For ease of comparison, the TOCs of ethanol measured by different methods and their error ranges are listed in Table 2 and plotted in Figure 7 (see Supplementary Section S5 for the details of the calculations). Compared with the value $(-3.99 \pm 0.20) \times 10^{-4}$ ℃$^{-1}$ presented in the literature[34] and another value $(-4.28 \pm 0.08) \times 10^{-4}$ ℃$^{-1}$ measured by us using the Fresnel reflection method over the temperature range of 18–56 ℃ (see Supplementary Section S6), the TOC determined by the UFOFC method is consistent with the reference data, whereas that determined by the OSA method is not.

In this experiment, we intentionally chose a small range of temperature change (0.1 ℃). One reason is to clearly demonstrate the advantage of fine resolution of the UFOFC method. The other reason is that the TOC itself is also temperature dependent (although only weakly).[35,36] Because they were limited by spectral resolution, many previous studies used a large temperature range (e.g., $\Delta T \sim 20$ ℃ in Ref. 34), and the TOC obtained in such studies is in fact the value averaged over that temperature range. By contrast, the UFOFC method enables measuring the value of the TOC very close to a specific temperature point.

Dynamic response

To examine the dynamic response of the UFOFC method, the DUT is replaced by a $LiNbO_3$ intensity modulator (Covega Mach-20 035, bandwidth 18 GHz). When an electrical pulse (with a width of 15 μs) is applied to the intensity modulator to generate a phase change pulse (see Figure 8a), the UFOFC method can detect the waveform very well (see Figure 8b). The rise and fall of the phase change are both captured within one cycle of data sampling, which is 8192/12 GHz = 0.7 μs (see Equation (S20)). This result demonstrates an enhancement in the response speed of greater than four orders of magnitude compared with the OSA sweep time (0.5 s).

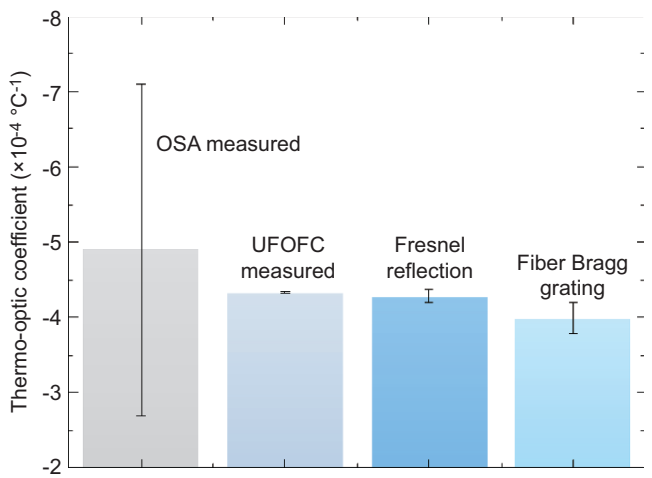

Figure 7 The thermo-optic coefficients and error ranges of ethanol measured by different methods.

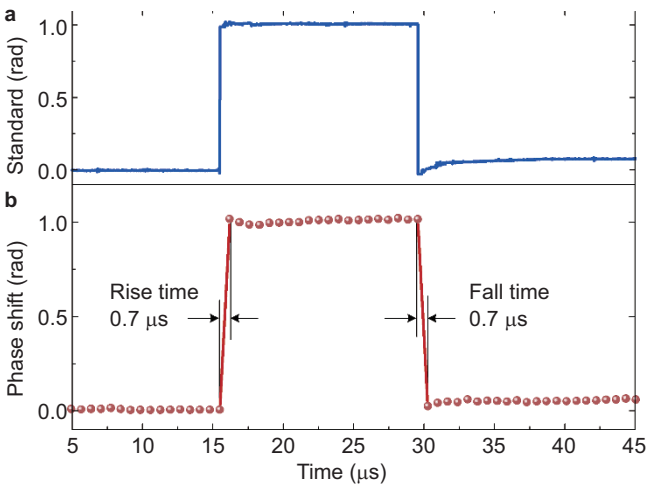

Figure 8 Dynamic response of the UFOFC method. In response to a pulse of standard phase change (**a**), the UFOFC can detect the phase change waveform (**b**). The rise time and fall time are both within one calculation cycle (0.7 μs).

DISCUSSION

The UFOFC method has capacity for further improvement. For instance, if a longer data length is used for the IFFT and FFT, the frequency spacing could be decreased to the Hz level and even lower, thereby enabling further improvement by more than six orders of magnitude. If the AWG has a faster sampling rate, the response time can be further reduced. Furthermore, thanks to the use of digital data processing, on the input side, the amplitude and phase of each comb line can be adjusted easily to generate arbitrary optical waveforms without the need for the complicated phase arrays that are used in other optical waveform generator.[37] On the output side, the amplitude, phase, and polarization of each comb line can be retrieved individually, which may enable detection of additional optical properties, such as polarization changes.

Nevertheless, the UFOFC has a potential problem of limited bandwidth of the frequency comb, e.g., only 10 GHz (~0.08 nm) in the experimental demonstration presented in this work. Such a limited bandwidth affects the measurement range of the spectral shift. This problem can be overcome by using a coarse frequency comb (e.g., with a spacing of 10 GHz and bandwidth 40 nm) as the light source. The generated ultrafine frequency combs can then automatically be stitched to span a large range (e.g., 40 nm).[27]

CONCLUSIONS

In summary, we have presented a method for generating UFOFCs and a niche application for high-resolution, fast spectral measurement. For an experimental demonstration, a frequency comb with a mode spacing of 1.46 MHz over the range of 10 GHz is generated by DSP and used to measure the tiny change in the refractive index of ethanol over a temperature range of only 0.1 ℃. Compared with the conventional method using optical spectrum analyzers, this UFOFC method has 167 times finer spectral resolution, 225 times smaller error, and 4 orders of magnitude faster dynamic response. The UFOFC method has the potential to boost the performance of many available optical sensors that require phase or spectral detection. Moreover, it can enable direct label-free optical detection of subtle biochemical responses in the time range of milliseconds to nanoseconds, which would be useful for measurements of binding kinetics, molecular dynamics, secretion and drug responses of cells and many other processes.[4,38–41]

ACKNOWLEDGMENTS

Zhaohui Li acknowledges the support of the National Basic Research Programme of China (973) (Project No. 2012CB315603), National High Technology 863 Research and Development Program of China (Nos. 2013AA013300 and 2013AA013403), the Research Fund for the Doctoral Program of Higher Education of China (20124401110003), National Natural Science Foundation of China (NSFC) (Grant No. 61435006), and the Program for New Century Excellent Talents in University (NCET-12-0679) in China. Xuming Zhang acknowledges the NSFC (Grant No. 61377068), the Hong Kong Research Grant Council (Grant Nos. PolyU 5327/11E and N_PolyU505/13) and the Hong Kong Polytechnic University (Grant Nos. G-YN07, 4-BCAL and G-YBBE).

1 White IM, Fan X. On the performance quantification of resonant refractive index sensors. *Opt Express* 2008; **16**: 1020–1028.
2 Vollmer F, Arnold S. Whispering-gallery-mode biosensing: label-free detection down to single molecules. *Nat Methods* 2008; **5**: 591–596.
3 Liang XJ, Liu AQ, Lim CS, Ayi TC, Yap PH. Determining refractive index of single living cell using integrated microchip. *Sens Actuators A* 2007; **133**: 349–354.
4 Song WZ, Zhang XM, Liu AQ, Lim CS, Yap PH *et al*. Refractive index measurement of single living cells using on-chip Fabry-Pérot cavity. *Appl Phys Lett* 2006; **89**: 203901.
5 Zhu J, Ozdemir SK, Xiao YF, Li L, He L *et al*. On-chip single nanoparticle detection and sizing by mode splitting in an ultrahigh-*Q* microresonator. *Nat Photon* 2010; **4**: 46–49.
6 Lackner M. *Gas Sensing in Industry by Tunable Diode Laser Spectroscopy (TDLS)*. Vienna, Australia: ProcessEng Engineering GmbH; 2008.
7 Dyroff C. *Tunable Diode-Laser Absorption Spectroscopy for Trace-Gas Measurements with High Sensitivity and Low Drift*. Karlsruhe, Germany: KIT Scientific; 2010.
8 Frish MB, Wainner RT, Laderer MC, Parameswaran KR, Sonnenfroh DM. Precision and Accuracy of Miniature Tunable Diode Laser Absorption Spectrometers. Proc. SPIE 8032, Next-Generation Spectroscopic Technologies IV, 803209, 2011.
9 Dale E, Liang W, Eliyahu D, Savchenkov AA, Ilchenko VS, Matsko AB. On Phase Noise of Self-injection Locked Semiconductor Lasers. Proc. SPIE 8960, Laser Resonators, Microresonators, and Beam Control XVI, 89600X, 2014.
10 Nunoya N, Ishii H, Iga R. High-speed tunable distributed amplification distributed feedback (TDA-DFB) lasers. *NTT Tech Rev* 2012; **10**: 1–7.
11 Newbury NR. Searching for applications with a fine-tooth comb. *Nat Photon* 2011; **5**: 186–188.
12 Udem T, Holzwarth R, Hänsch TW. Optical frequency metrology. *Nature* 2002; **416**: 233–237.
13 Ye J, Cundiff ST (eds.). *Femtosecond Optical Frequency Comb: Principle, Operation, and Applications*. Norwell, USA: Springer, 2005.
14 Bartels A, Heinecke D, Diddams SA. 10-GHz self-referenced optical frequency comb. *Science* 2009; **326**: 681.
15 Kippenberg TJ, Holzwarth R, Diddams SA. Microresonator-based optical frequency combs. *Science* 2011; **332**: 555–559.
16 Marian A, Stowe MC, Lawall JR, Felinto D, Ye J. United time-frequency spectroscopy for dynamics and global structure. *Science* 2004; **306**: 2063–2068.
17 Thorpe MJ, Ye J. Cavity-enhanced direct frequency comb spectroscopy. *Appl Phys B* 2008; **91**: 397–414.
18 Adler F, Thorpe MJ, Cossel KC, Ye J. Cavity-enhanced direct frequency comb spectroscopy: technology and applications. *Ann Rev Anal Chem* 2010; **3**: 175–205.
19 Fleisher AJ, Bjork BJ, Bui TQ, Cossel KC, Okumura M. Mid-infrared time-resolved frequency comb spectroscopy of transient free radicals. *J Phys Chem Lett* 2014; **5**: 2241–2246.
20 Foltynowicz A, Ban T, Masłowski P, Adler F, Ye J. Quantum-noise-limited optical frequency comb spectroscopy. *Phys Rev Lett* 2011; **107**: 233002.
21 Diddams SA, Hollberg L, Mbele V. Molecular fingerprinting with the resolved modes of a femtosecond laser frequency comb. *Nature* 2007; **445**: 627–630.
22 Mandon J, Guelachvili G, Picqué N. Fourier transform spectroscopy with a laser frequency comb. *Nat Photon* 2009; **3**: 99–102.
23 Ideguchi T, Holzner S, Bernhardt B, Guelachvili G, Picqué N *et al*. Coherent Raman spectro-imaging with laser frequency combs. *Nature* 2013; **502**: 355–358.
24 Ideguchi T, Poisson A, Guelachvili G, Picqué N, Hänsch TW. Adaptive real-time dual-comb spectroscopy. *Nat Comm* 2014; **5**: 3375.
25 Li J, Li Z. Frequency-locked multicarrier generator based on a complementary frequency shifter with double recirculating frequency-shifting loops. *Opt Lett* 2013; **38**: 359–361.
26 Yi X, Li Z, Bao Y, Qiu K. Characterization of passive optical components by DSP-based optical channel estimation. *IEEE Photon Technol Lett* 2012; **24**: 443–445.
27 Jin C, Bao Y, Li Z, Gui T, Shang H *et al*. High-resolution optical spectrum characterization using optical channel estimation and spectrum stitching technique. *Opt Lett* 2013; **38**: 2314–2316.
28 Betzler K, Gröne A, Schmidt N, Voigt P. Interferometric measurement of refractive indices. *Rev Sci Instrum* 1988; **59**: 652–653.
29 Tian Z, Yam SS, Barnes J, Bock W, Greig P *et al*. Refractive index sensing with Mach–Zehnder interferometer based on concatenating two single-mode fiber tapers. *IEEE Photon Technol Lett* 2008; **20**: 626–628.
30 Schubert T, Haase N, Kück H, Gottfried-Gottfried R. Refractive-index measurements using an integrated Mach-Zehnder interferorneter. *Sens Actuators A* 1997; **60**: 108–112.
31 Qi ZM, Matsuda N, Itoh K, Murabayashi M, Lavers CR. A design for improving the sensitivity of a Mach-Zehnder interferometer to chemical and biological measurands. *Sens Actuators B* 2002; **81**: 254–258.
32 Wang Y, Yang M, Wang DN, Liu S, Lu P. Fiber in-line Mach–Zehnder interferometer fabricated by femtosecond laser micromachining for refractive index measurement with high sensitivity. *J Opt Soc Am B* 2010; **27**: 370–374.
33 Liu Q, Tu X, Kim KW, Kee JS, Shin Y *et al*. Highly sensitive Mach–Zehnder interferometer biosensor based on silicon nitride slot waveguide. *Sens Actuators B* 2013; **188**: 681–688.
34 Kamikawachi RC, Abe I, Paterno AS, Kalinowski HJ, Muller M *et al*. Determination of thermo-optic coefficient in liquids with fiber Bragg grating refractometer. *Opt Commun* 2008; **281**: 621–625.
35 Kim YH, Park SJ, Jeon SW, Ju S, Park CS *et al*. Thermo-optic coefficient measurement of liquids based on simultaneous temperature and refractive index sensing capability of a two-mode fiber interferometric probe. *Opt Express* 2012; **20**: 23744–23754.
36 Ghosh G. *Handbook of Thermo-optic Coefficients of Optical Materials with Applications*. San Diego, USA: Academic Press, 1998.
37 Ye J. Optical metrology: everything under control. *Nat Photon* 2007; **1**: 447–448.

38 Lin VS, Motesharei K, Dancil KP, Sailor MJ, Ghadiri MR. A porous silicon-based optical interferometric biosensor. *Science* 1997; **278**: 840–843.
39 Hou BH, Takanaga H, Grossmann G, Chen LQ, Qu XQ *et al*. Optical sensors for monitoring dynamic changes of intracellular metabolite levels in mammalian cells. *Nat Protoc* 2011; **6**: 1818–1833.
40 Oh KJ, Cash KJ, Plaxco KW. Beyond molecular beacons: optical sensors based on the binding-induced folding of proteins and polypeptides. *Chem* 2009; **15**: 2244–2251.
41 Fang Y. Label-free cell-based assays with optical biosensors in drug discovery. *Assay Drug Dev Technol* 2006; **4**: 583–595.

Supplementary Information for this article can be found on *Light: Science & Applications*' website (http://www.nature.com/lsa).